JMEPEG (2010) 19:572–584
DOI: 10.1007/s11665-009-9503-x

1059-9495/$19.00

The Effects of Martensite Content on the Mechanical Properties of Quenched and Tempered 0.2%C-Ni-Cr-Mo Steels

John M. Tartaglia

(Submitted February 13, 2009; in revised form June 2, 2009)

Three martensite contents (approximately 35, 50, and 100%) were obtained in a SAE8822 steel by altering the quenching media and section size. Another variation in martensite content (approximately 80 versus 97%) was achieved by quenching a SAE8622 steel in the same section size. The impact toughness and fatigue properties were determined after tempering to various levels of monotonic strength. Toughness and strength-toughness combinations improved with increased as-quenched martensite contents at all levels of as-tempered ultimate tensile strength (UTS). Even at higher levels of yield strength (YS), increased martensite contents produced higher impact energies and lower fracture appearance transition temperatures. The cyclic YS was independent of martensite content (at the same level of UTS), even though the monotonic YS increased with martensite content. When fatigue test results were compared at a tensile strength of 1240 MPa (180 ksi), actual and predicted fatigue lives in the high cycle regime increased with martensite content, but low cycle fatigue resistance was relatively unaffected. Fatigue strength and UTS were directly related, and all the quenched and tempered steels exhibited cyclic softening.

Keywords carbon/alloy steels, heat treating, material selection, mechanical testing, optical microscopy

1. Introduction

Quenched and tempered (Q&T) steels are widely used in structural applications. Depending on the alloy content of the steels and the section size of the part being quenched, various microstructures will be obtained in the as-quenched condition. Higher alloy contents and decreasing section sizes (increasing cooling rates) promote the formation of martensite versus bainite, pearlite, and ferrite, which form at higher temperatures. After quenching, hardened steels are usually tempered to improve ductility and toughness, with a concomitant loss in strength.

Q&T product specifications commonly omit microstructural requirements in the as-quenched condition. Usually the specifications contain only the yield strength (YS), tensile strength, or hardness in the Q&T condition. However, the as-quenched microstructure is important because it can affect other properties, such as toughness and fatigue resistance, in the as-tempered condition. Numerous component failures have resulted from steel heat treatments that effect acceptable tensile properties, but toughness and fatigue resistance are too low due to the presence of nonmartensitic constituents in the as-quenched condition. When hardened steels contain other constituents besides martensite, they are often called "slack quenched."

The toughness of tempered steels is strongly affected by the microstructure in the hardened state. For example, the Charpy V-Notch (CVN) impact toughness of a 0.7%Cr-0.32%Mo steel was compared at four different carbon contents and four different microstructures in the as-hardened condition (Ref 1). After tempering to the same hardness, the ductile-to-brittle impact transition temperature for any carbon level was 25-50 °C (45-90 °F) lower for fully martensitic microstructures than for microstructures containing only 50% martensite. This author and others have shown that SAE 4340 steel has better impact toughness when it is austempered (isothermally transformed) to 100% lower bainite than when it is quenched to 100% martensite and tempered to the same strength level (Ref 1, 2). However, steels with mixed microstructures resulting from incomplete bainitic treatments and partial transformation to martensite possess much lower toughness (higher transition temperatures) than steels with microstructures containing either 100% lower bainite or 100% tempered martensite (Ref 1).

Microstructure also influences the high cycle fatigue resistance of medium carbon steels. Martensitic steels give better high cycle fatigue resistance than ferrite-pearlite steels whereas microstructures resulting in good long-life fatigue resistance will generally give lower thresholds for crack growth (Ref 3). Borik et al. (Ref 4) evaluated the fatigue strength of five medium carbon alloy steels in the 10^5 to 10^8 cycle range. The steels were continuously cooled (rather than isothermally transformed) to various as-quenched martensite contents and tempered to 36 Rockwell C hardness (HRC). These investigators found that the fatigue limits decreased as the martensite content decreased from 100 to 85%; however, further decreases in the martensite content did not lower fatigue resistance more (Ref 4).

John M. Tartaglia, Stork Climax Research Services, 51229 Century Court, Wixom, MI 48393. Contact e-mail: john.tartaglia@stork.com.

Landgraf (Ref 5) reviewed the influence of microstructure on the fatigue properties of ferrous alloys. As a class of materials, Q&T martensitic steels exhibit cyclic softening (except for ausformed and quenched steels). Maximum softening occurs in quenched and tempered SAE1045 steel at Brinell hardness values between 225 and 600, and cyclic stability (equivalent monotonic and cyclic offset yield strengths) occurs at both hardness extremes (Ref 5). The mechanisms influencing such complex fatigue behavior have been discussed both by Landgraf (Ref 5) and by Stoloff and Duquette (Ref 6).

Although the influence of as-quenched microstructure on toughness and high cycle fatigue resistance has been evaluated extensively, as-quenched microstructural effects on low cycle fatigue properties have not been investigated. In this study, SAE8622 and SAE8822 steels were quenched to produce various martensite contents and tempered to various ultimate tensile strengths. The effects of martensite content on fatigue resistance and toughness were then evaluated.

2. Experimental Procedures

2.1 Materials

One 57 kg (125 lb) laboratory heat was cast for each of three compositions. Each heat was induction-melted in air, aluminum-killed, and poured into two 130 mm (5.25 in.) diameter by 220 mm (8.63 in.) long molds. Table 1 shows the compositions for the three heats; the compositions were determined from button specimens on an integral part of one of the ingots per heat. Steel 2 meets the midrange of the chemical requirements for SAE8622 steel, which contains a maximum of 0.25%Mo. Steels 1A and 1B meet the requirements for SAE8822 steel, which is a high molybdenum modification of SAE8622 steel.

The ingots were forged into cylindrical bars in the temperature range of 1065-1205 °C (1950-2200 °F). One 32 mm (1.25 in.) diameter bar and a number of bars with diameters between 27 and 29 mm (1.06 and 1.13 in.) were forged for each steel. A number of 19 mm (0.75 in.) bars of Steel 1A were forged and rolled in the same temperature range.

2.2 Heat Treatment

All the bar stock was annealed by austenitizing at 925 °C (1700 °F) and furnace cooling. The 32 mm (1.25 in.) diameter bars were machined into standard Jominy end-quench specimens. The 27-29 mm (1.06-1.13 in.) and 19 mm (0.75 in.) diameter bars were machined to diameters of 25 and 17 mm (1.00 and 0.65 in.), respectively, and cut to various lengths. These latter bars were austenitized at 845 °C (1550 °F) for 1 h before quenching in either water or oil. Some bars were tempered for 2 h at temperatures between 205 and 650 °C (400 and 1200 °F), and these bars were air-cooled after tempering. Mechanical test blanks were machined from these quenched and Q&T bars.

Bars of Steel 1A were subjected to quenching treatments that produced three levels of martensite. The different martensite levels were obtained by varying the section size [17 mm (0.65 in.) versus 25 mm (1.0 in.) diameter] and quenching media (water versus oil). The hardened bars were then tempered to ultimate tensile strengths between 869 and 1138 MPa (126 and 165 ksi). This series of specimens provided a comparison of different microstructures while maintaining constant composition.

Bars of Steels 1B and 2 were water quenched in the 25 mm (1.0 in) section size and tempered (for 2 h) to a ultimate tensile strength (UTS) of 1240 MPa (180 ksi). This series of specimens provided a comparison of different microstructures obtained by alloying effects (0.20 versus 0.37%Mo) on hardenability.

2.3 Hardness and Metallography

Rockwell hardness (HRC) was determined as the average of three readings taken near the centers of transverse sections of the heat-treated bars in accordance with ASTM standard E18. The conversions shown in ASTM standard A370 were used to select the tempering conditions that would result in the desired UTS value. Rockwell C hardness measurements were also used to ensure uniform quenching in the longitudinal bar direction.

An approximate martensite content was assigned to each alloy/quench condition based on as-quenched hardness. Measuring martensite contents using quantitative metallographic techniques is extremely difficult and time consuming, but quantitative microstructural analysis does not guarantee accurate results. Admittedly, martensite contents assigned by hardness are decidedly approximate. The hardness method used in this study for assigning martensite contents is deemed adequate, because quantitative correlations of various mechanical properties with martensite content were not attempted.

A transverse metallographic specimen was prepared for selected heat treatment conditions. Each piece was mounted and mechanically polished. The metallographic specimens were etched in 4 g picric acid and 1 mL nitric acid in 95 mL ethanol (4PIN) and photographed using an optical metallograph.

The retained austenite was measured by x-ray diffraction, and a Vickers hardness (HV10) gradient was obtained with a 10-kg load in accordance with ASTM standard E92 on transverse sections from the undeformed shoulders of some fractured tensile specimens. At least two hardness readings were obtained at each radial position.

Table 1 Compositions of test steels, wt.%

											Al	
Steel	**Heat no.**	**C**	**Mn**	**Si**	**Ni**	**Cr**	**Mo**	**P**	**S**	**N**	**Total**	**Acid soluble**
1A	6530	0.23	0.81	0.22	0.51	0.51	0.36	0.017	0.018	0.012	0.036	ND
1B	6429	0.21	0.82	0.24	0.55	0.50	0.38	0.013	0.017	0.013	0.094	0.075
2	6428	0.21	0.82	0.27	0.54	0.50	0.20	0.017	0.017	0.0152	0.091	0.071

ND, not determined

The prior austenite grain sizes of all the steels were determined from small pieces austenitized at 925 °C (1700 °F) for 1 h and water quenched. After the quenched pieces were tempered at 230 °C (450 °F) for 3 days, transverse sections were cut and metallographically prepared. After etching with saturated aqueous picric acid reagents, the prior austenite grain sizes were determined by the linear intercept method in accordance with ASTM standard E112.

2.4 Jominy End-Quench Tests

Jominy end-quench tests were performed for each steel in accordance with ASTM standard A255. The Jominy specimens were austenitized at 925 °C (1700 °F) for 30 min prior to end quenching. Two bars were tested for Steel 1A and one was tested for each of Steels 1B and 2. After quenching, parallel flats were surface ground on opposite sides of each bar, and Rockwell hardness (HRC) was determined as a function of distance from the quenched end.

Values for the ideal critical diameter (D_I), the diameter of a cylindrical steel bar which will form 50% martensite at its center when subjected to an ideal quench, were determined experimentally from each Jominy curve using the hardness drop method (Ref 7). D_I values for each steel were also calculated from known alloying contributions (Ref 7, 8).

2.5 Tensile Tests

Tensile specimens were prepared from heat-treated bars and tested at room temperature on a screw-driven tensile machine in accordance with ASTM standard E8. The specimens had gauge sections that were 6.3 mm (0.25 in.) in diameter and 25 mm (1 in.) in length. Strain rates of 18 and 300%/h were used in the elastic and plastic ranges, respectively. At least two specimens were tested for each alloy/heat treatment combination. The quench and temper treatments, which produced the desired ultimate tensile strengths, were selected for further mechanical property evaluation.

2.6 Charpy V-Notch Impact Tests

Standard CVN impact specimens were prepared for each alloy/heat treatment combination that achieved the desired strength levels. The impact energy and per cent shear fracture were determined in accordance with ASTM standard E23, as a function of test temperature.

2.7 Fatigue Tests

Fatigue specimens were prepared for a selected number of the alloy/heat treatment combinations which resulted in the desired ultimate strengths. The cylindrical specimens possessed gauge sections that were 19 mm (0.75 in.) in length and 6.4 mm (0.25 in.) in diameter. The specimens were prepared such that no heating of the gauge sections occurred; the gauge sections were polished by machine to a ~0.05 μm (~2 μ-in.) finish.

Fully reversed fatigue tests were performed at room temperature on a servohydraulic fatigue machine in accordance with ASTM standard E606. A longitudinal extensometer was mounted on each specimen. The tests were performed in strain control at constant strain rates of 0.005/s for Steel 1A and 0.01/s for Steels 1B and 2. Total strain and load were recorded throughout each test, and load-strain hysteresis loops were generated for the first few cycles. The saturation stress ($\Delta\sigma/2$) and actual total strain ($\Delta\varepsilon_T/2$) amplitudes were measured at half-life, i.e., one-half the number of cycles to failure (N_f) defined as specimen fracture. The elastic modulus (E) of each specimen was obtained from the first quarter cycle (monotonic stress-strain curve). For applied total strain amplitudes less than ±0.3%, fatigue tests were performed in strain control until saturation was reached, i.e., until the load amplitude remained constant. These low cyclic strain tests were then continued in load control using a 30-Hz sinusoidal waveform until failure was reached, thereby minimizing machine time.

The plastic strain amplitude ($\Delta\varepsilon_p/2$) and fatigue life regression constants (σ_f', b, ε_f', and c) were evaluated using the procedures outlined in ASTM standard E606 and the Appendix of this paper. For Steels 1B and 2, the cyclic strength coefficient (K') and cyclic strain hardening exponent (n') were calculated (see Appendix) using the saturation stress and plastic strain amplitudes obtained from the strain-life tests. However, for Steel 1A, these parameters were obtained using incremental step tests (ISTs) (Ref 9).

The ISTs were performed in fully reversed strain control using a constant strain rate of 0.01/s. The specimens were cycled once at ±1.5, ±1.4, ±1.3,…, ±0.2, and ±0.1 total strain amplitudes resulting in fifteen ±0.1% strain increments for each "unloading" IST block. The specimens were then reloaded starting with ±0.1% total strain amplitude and continuing in a similar progression to ±1.5% total strain amplitude. The entire process was repeated until the cyclic stress-strain curve (on unloading) was stabilized, i.e., when no changes in the load-strain values between the last two unloading IST blocks were observed. Load-time plots, strain-time plots, and load-strain hysteresis loops were generated throughout each test. The last unloading IST block was analyzed for the cyclic stress-strain curve parameters (K' and n') at saturation.

The monotonic strength coefficient (K) and strain hardening exponent (n) were also obtained for all the fatigue test conditions. These quantities were calculated (see Appendix) using the monotonic true stress and true plastic strain values obtained from the first loading to ±1.5% strain in either a strain-life or IST. These K and n determination procedures are essentially equivalent to those contained in ASTM standard E646 for tensile tests.

3. Results

3.1 End-Quench Hardenability

The Jominy end-quench hardenability curves and ideal critical diameters obtained for the three steels are shown in Fig. 1. Steel 2 has lower hardenability than Steels 1A and 1B, as would be expected from the higher molybdenum contents of the latter two steels. The ideal critical diameters calculated using known alloy factors (Ref 7, 8) are in good agreement with those determined experimentally from the Jominy curves using the hardness drop method (Ref 7) as reported in Fig. 1.

3.2 Microstructure and Hardness

Table 2 shows the center hardness of the bars for each steel/quench condition. The last column of Table 2 shows the

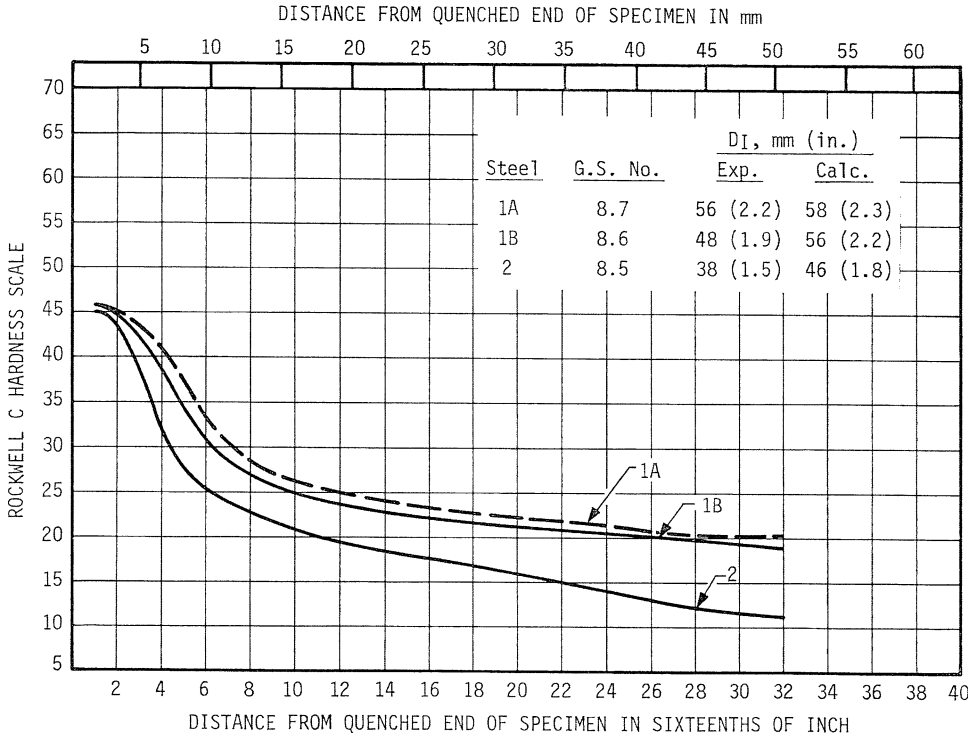

Fig. 1 Jominy end-quench hardenability curves of steels austenitized at 925 °C (1700 °F)

Table 2 Hardness and tensile properties in as-quenched conditions

Steel	% Mo	Bar diameter, mm	Bar diameter, in	Quenchant	Center hardness HRC	Center hardness HV10	YS MPa	YS ksi	UTS MPa	UTS ksi	% RA	% El	% Martensite at bar center
1A	0.36	17	0.65	Water	47.0	503	1213	176	1579	229	43	11	100
1A	0.36	17	0.65	Oil	33.4	345	786	114	1138	265	52	14	50
1A	0.36	25	1	Oil	31.0	309	696	101	993	144	56	16	35
1B	0.38	25	1	Water	42.3	427	1110	161	1420	206	43	12	97
2	0.20	25	1	Water	37.3	377	848	123	1172	170	43	14	80

martensite contents obtained at the centers of the quenched pieces. These martensite contents were assigned by interpolation and extrapolation of the hardness data of Hodge and Orehoski (Ref 10). Steel 1A was fully hardened in the water-quenched condition. Its hardness is in excellent agreement with the hardness obtained by Hodge and Orehoski (Ref 10) at a distance of 1.6 mm (1/16 in.) from the quenched end of Jominy bars, as well as the fully martensitic hardness values obtained by several other investigators as compiled by Krauss (Ref 11).

The three different contents of martensite assigned for Steel 1A using hardness measurements for the three quench conditions are in good qualitative agreement with the microstructures of this steel. Figure 2(a) shows that the microstructure consists entirely of lath martensite. However, mixtures of martensite and bainite are shown in Fig. 2(b) and (c). Using hardness data, these latter views were assigned respective martensite contents of 50 and 35%.

Differing martensite contents were also obtained by varying alloy contents. Table 2 and Fig. 3 show that when Steels 1B (0.38%Mo) and Steel 2 (0.2%Mo) were quenched in the same 25 mm (1 in.) section size, more martensite was obtained in Steel 1B. Figures 2(a) and 3(a), respectively, show that a slight difference in martensite content was observed between Steels 1A and 1B when water quenched. Figure 1 shows that these two steels have almost identical hardenability. The 8 mm (0.35 in.) difference in section size accounts for the difference in martensite content at the center of the bars, i.e., Steels 1A and 1B were water quenched in 17 and 25 mm (0.65 and 1.0 in) diameter sections, respectively.

Figures 4 and 5 show optical micrographs corresponding to five of the six quench and temper conditions (see Table 3) evaluated in this study. Figures 4(a) and 5(a) illustrate the substantial difference in martensite morphology that is obtained when fully, or nearly fully as-quenched martensite is tempered at temperatures that differ by 222 °C (400 °F).

3.3 Tensile Properties

Table 2 shows the effect of martensite content on tensile properties in the as-quenched condition. The 0.2% offset YS and UTS values all decreased substantially as the martensite content (hardness) decreased. Ductility, as measured by percent

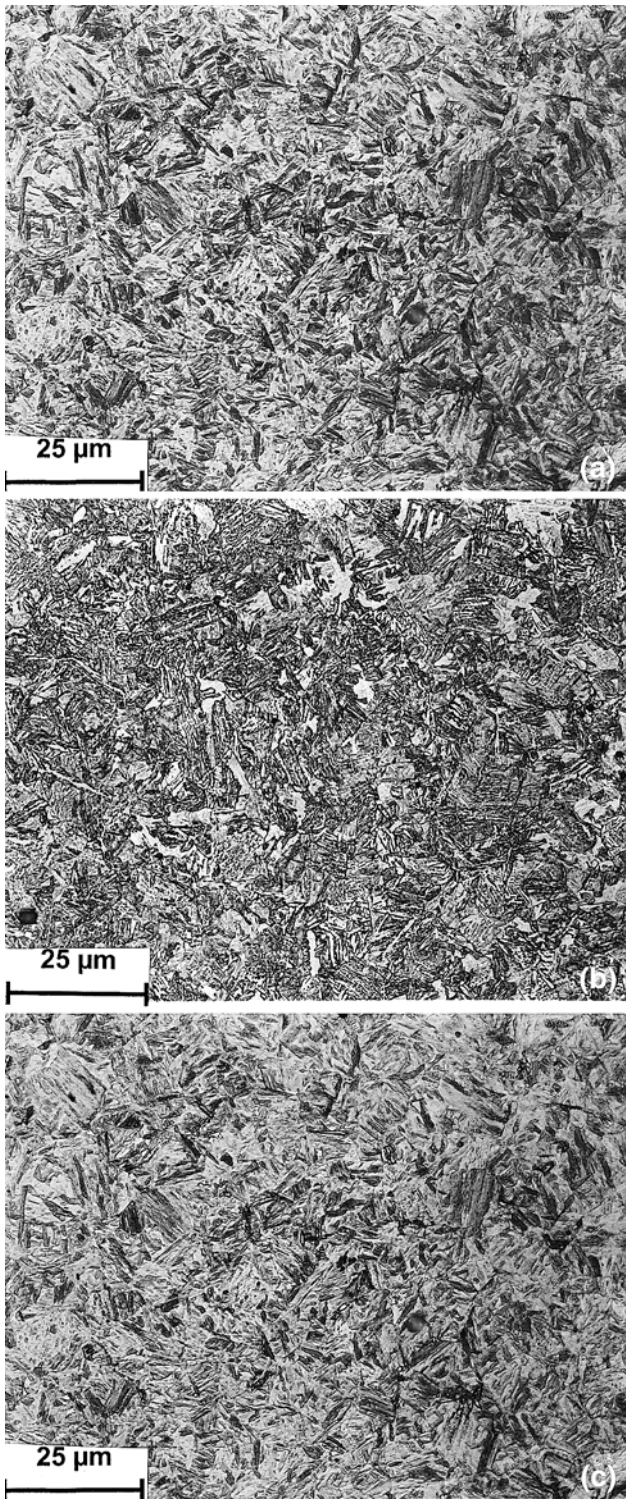

Fig. 2 As-quenched microstructures of Steel 1A bar centers. (a) Water quenched 17 mm (0.65 in.), diameter section—100% martensite. (b) Oil quenched 17 mm (0.65 in.), diameter section—50% martensite. (c) Oil quenched 25 mm (1 in.), diameter section—35% martensite

reduction of area (%RA), was identical for martensite contents above 80% and increased slightly with lower martensite contents. The percent elongation (%El) also increased slightly with decreasing martensite content.

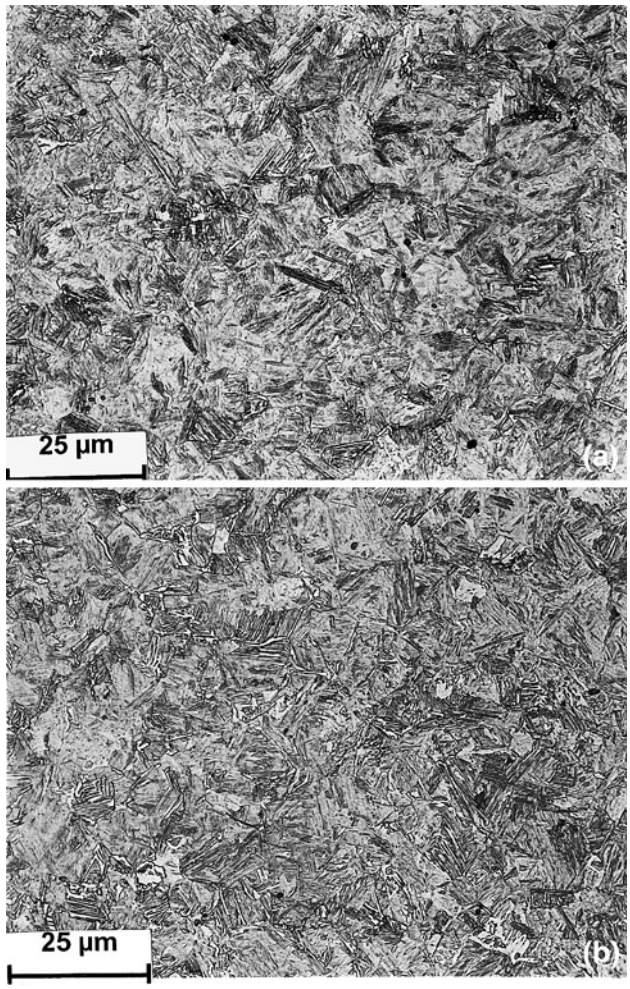

Fig. 3 As-quenched microstructures at centers of water quenched 25 mm (1 in.), diameter bar sections. (a) Steel 1B (0.38% Mo)—97% martensite. (b) Steel 2 (0.2% Mo)—80% martensite

Figure 6 shows the effect of tempering temperature on the YS for all the steels and quenching treatments. For the specimens with the 100% as-quenched martensite content and tempered only at temperatures above 540 °C (1000 °F), the YS decreased with increasing tempering temperature. After tempering at temperatures up to about 350 °C (660 °F), the as-tempered YS was higher than its respective as-quenched value for all the other conditions. For the 50 and 97% as-quenched martensite contents, the yield strengths decreased with increasing tempering temperature after reaching a maximum value at an intermediate tempering temperature.

Figure 7 shows that only Steel 2, tempered at much lower temperatures than the other four steel/quench combinations, exhibited a higher UTS in the as-tempered versus the as-quenched condition. After quenching to 35 and 50% martensite contents and tempering at temperatures below 425 °C (800 °F), Steel 1A exhibited no loss in tensile strength versus the as-quenched condition. At the two highest martensite contents (97 and 100%), similar slopes for the UTS versus tempering temperature curves were obtained.

Table 3 shows the conditions selected for further property evaluation. For Steel 1A, the tempering treatments that resulted in UTS values nearest 965 MPa (140 ksi) were chosen for the

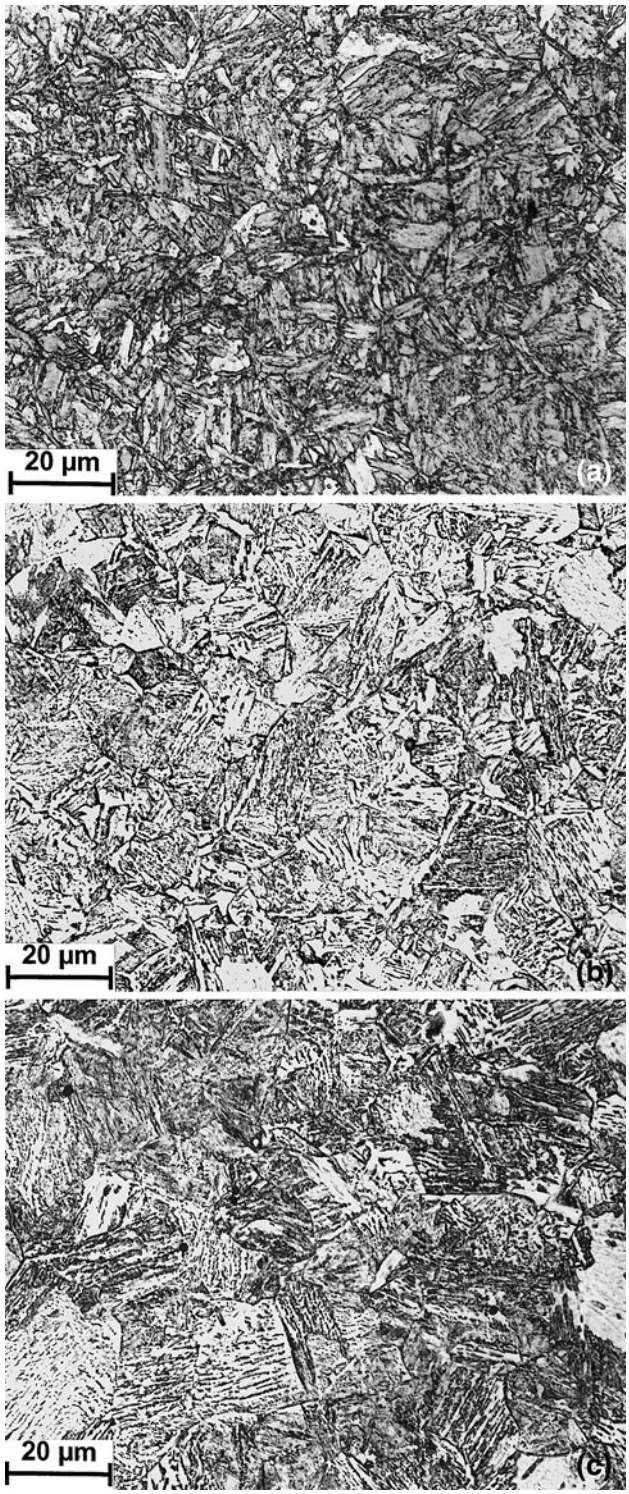

Fig. 4 As-tempered microstructures of Steel 1A at bar centers. (a) 100% Martensite—tempered at 593 °C (1100 °F). (b) 50% Martensite—tempered at 399 °C (750 °F). (c) 35% martensite—tempered at 371 °C (700 °F)

35 and 100% as-quenched martensite contents. For the Steel 1A-50% martensite condition, two tempering temperatures that resulted in higher and lower UTS values were chosen. For Steels 1B and 2, the tempering treatments that resulted in UTS values nearest 1240 MPa (180 ksi) were chosen.

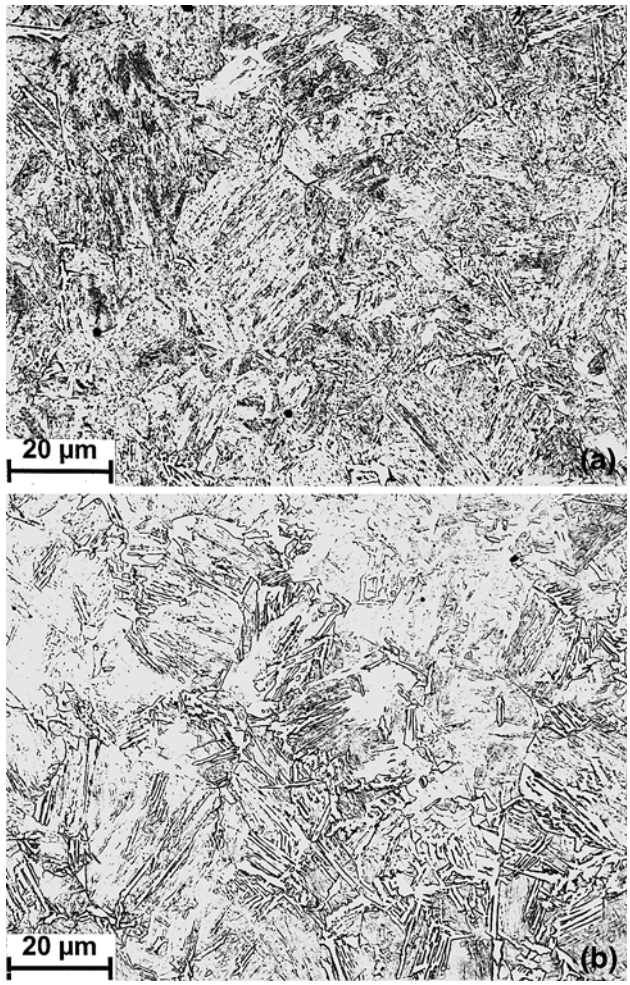

Fig. 5 As-tempered microstructures of Steels 1B and 2 at bar centers. (a) Steel 1B (0.38%Mo)—97% martensite, tempered at 371 °C (700 °F). (b) Steel 2 (0.2%Mo)—80% martensite, tempered at 204 °C (400 °F)

Except for the two 50% martensite conditions, where two different tempering temperatures were studied, the conditions will be identified by only the martensite content in most of the remainder of this paper. However, it should be noted that the various martensite contents were obtained by both variations in alloy content and quenching procedures, and more than one UTS level was evaluated in this study.

3.4 Impact Toughness

Figure 8 shows the CVN impact transition curve obtained after tempering for Steel 1A. Figure 9 shows the CVN results for Steels 1B and 2. Each impact energy data point represents the results of one test. Table 4 shows the fracture appearance transition temperature (FATT) for each condition tested.

As the as-quenched martensite content in Steel 1A was increased from 35 to 100% at a constant UTS, the toughness increased substantially. The absorbed energies more than doubled and the FATT decreased by 145 °C (260 °F). When the toughness of the 50% martensite condition [UTS = 1144 MPa (166 ksi)] was compared to that of the 35% martensite condition [UTS = 944 MPa (137 ksi)], little difference in the impact energy curves was observed. However, the

Table 3 Hardness and tensile properties after tempering

Steel	Mo, %	Martensite at bar center, %	Tempering temperature °C	Tempering temperature °F	Center hardness HRC	Center hardness HV10	YS MPa	YS ksi	UTS MPa	UTS ksi	RA, %	El, %
1A	0.36	100	593	1100	28.4	292	896	130	972	141	60	18
1A	0.36	50	399	750	31.0	330	1007	146	1144	166	58	16
1A	0.36	50	538	1000	24.1	280	745	108	869	126	67	23
1A	0.36	35	371	700	30.2	340	758	110	944	137	60	16
1B	0.38	97	371	700	39.5	400	1124	163	1255	182	58	16
2	0.20	80	204	400	36.8	371	972	141	1275	185	43	12

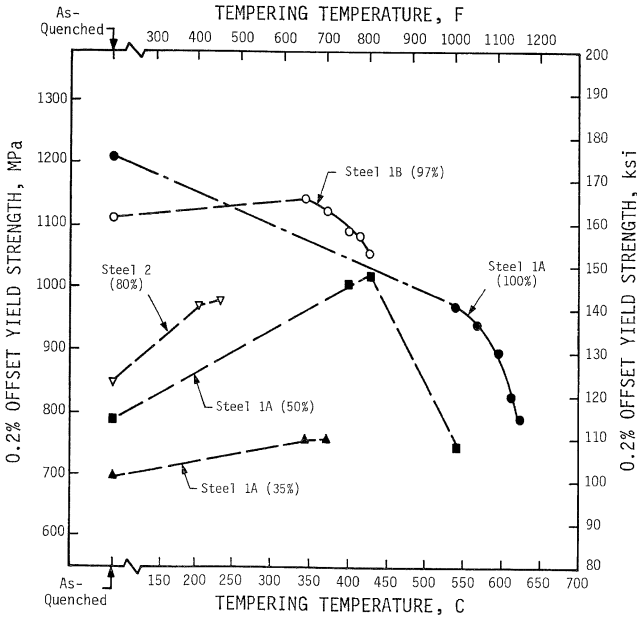

Fig. 6 Yield strength vs. tempering temperature. Numbers in parentheses are martensite contents

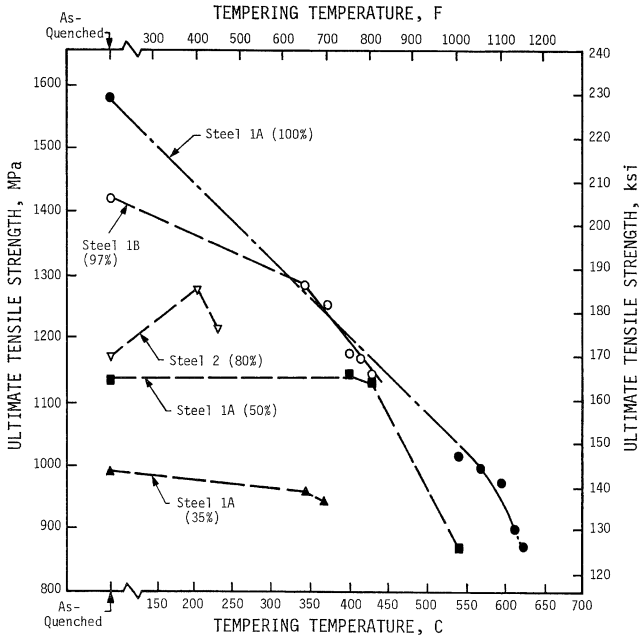

Fig. 7 Ultimate tensile strength vs. tempering temperature. Numbers in parentheses are martensite contents

FATT was 17 °C (30 °F) lower for the higher strength—50% martensite condition. Although the comparison is based on limited data for the 50% martensite—869 MPa (126 ksi) tensile strength condition, higher toughness was still obtained for the 100% martensite condition exhibiting the higher 972 MPa (141 ksi) UTS.

Figure 9 and Table 4 show a relatively small increase in toughness when the martensite content was increased from 80 to 97% by adding molybdenum. The FATT for the 97% martensite content was 28 °C (50 °F) higher at the 1240 MPa (180 ksi) UTS level.

3.5 Fatigue Properties and Strain Hardening Behavior

Figure 10(a) shows the experimental results (total strain amplitude versus reversals) of the strain-life fatigue testing obtained after tempering. Figures 10(b) and (c) show how the total strain amplitude was resolved into its plastic strain and stress (elastic strain) components versus reversals. Table 5 shows the fatigue life constants obtained by linear regression. Table 6 shows the calculated lives at selected strain levels using these constants. All the fatigue life calculations were performed with an elastic modulus (E) of approximately 200 GPa (30 million psi) that was obtained for the four test conditions.

Figure 10 and Table 6 show that microstructure, alloy content, and monotonic strength did not significantly influence low cycle fatigue life. However, higher UTS resulted in significantly higher lives at total strain amplitudes less than ±0.45%. Although martensite content did not affect the high cycle fatigue resistance at the 965 MPa (140 ksi) UTS level, Table 6 shows that the calculated fatigue life at the ±0.25% total strain amplitude increased as the martensite content was raised by adding more molybdenum at the 1240 MPa (180 ksi) UTS level.

Table 7 shows the monotonic and cyclic strain hardening constants obtained for the Q&T steels. Figure 11 shows the stress-strain curves calculated using these constants.

4. Discussion

For most applications of alloy steels that are hardened by allotropic transformation, a tempering operation is performed after quenching. The primary purpose of the tempering process is to increase impact toughness to the level necessary for the given application, usually at the expense of a slight reduction in

strength. The choice of tempering temperature is governed by the as-quenched content since this microstructural parameter has the strongest influence on the as-quenched strength and hardness of a particular steel. This research program evaluated the effect of martensite content on the strength, toughness, fatigue resistance, and strain hardening response obtained after tempering.

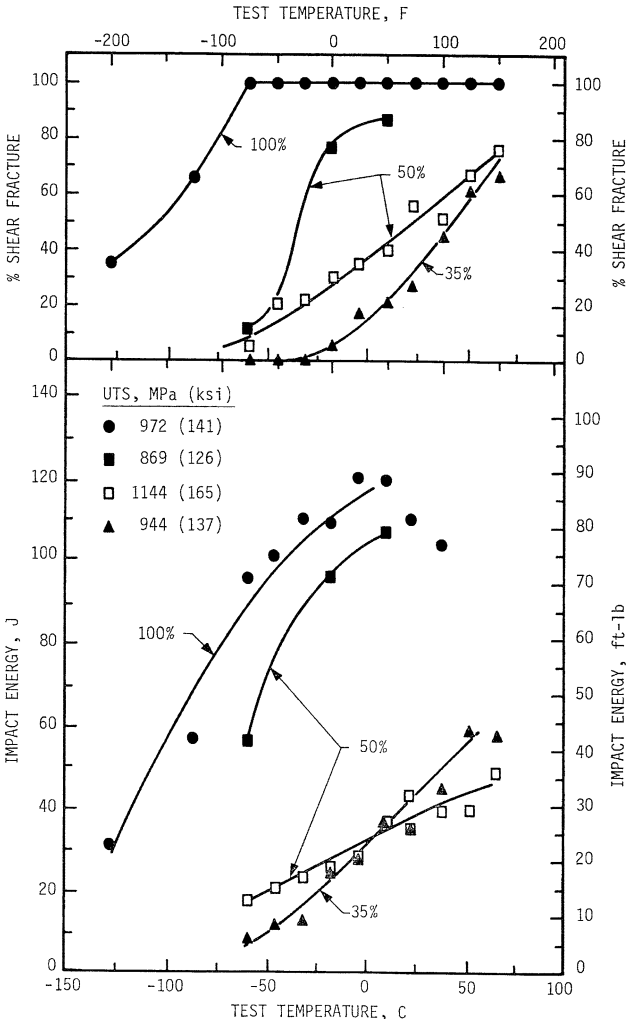

Fig. 8 CVN impact transition curves for Steel 1A in the quenched and tempered condition. Numbers in parentheses are martensite contents

4.1 Monotonic Strength After Tempering

Strength usually decreases when alloy steels are tempered. However, Fig. 6 shows that the YS increased after tempering for selected conditions evaluated in this study.

Previously, the phenomenon of higher as-tempered versus as-quenched flow strength has been noted for martensitic Fe-0.2C alloys (Ref 12-14). The rise in elastic limit from very low values in as-hardened steel to much higher values after tempering in the range of 260-370 °C (500-698 °F) has been attributed (Ref 12, 14) to internal transformational stresses generated on hardening. Investigators suggested that these stresses, which have tensile components in the direction of tensile loading, promote localized yielding and thereby cause an effective lowering of the elastic limit. The lower elastic limit

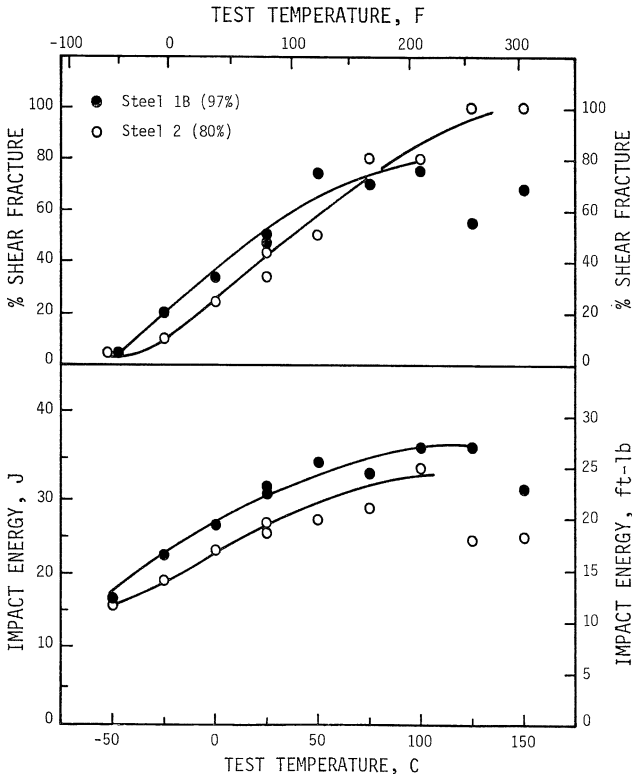

Fig. 9 CVN impact transition curves for Steels 1B (0.38%Mo) and 2 (0.2%Mo) quenched and tempered to UTS ≅1240 MPa (180 ksi). Numbers in parentheses are martensite contents

Table 4 Charpy V-Notch toughness of quenched and tempered steels

Steel	Mo, %	Martensite at bar center in as-quenched condition, %	Tempering temperature		UTS		Maximum impact energy,		FATT	
			°C	°F	MPa	ksi	J	ft-lb	°C	°F
1A	0.36	100	593	1100	972	141	121	89	−104	−155
1A	0.36	50	399	750	1144	166	49	36	24	75
1A	0.36	50	538	1000	869	126	107	79	≈−34	≈−30
1A	0.36	35	371	700	944	137	60	44	41	105
1B	0.38	97	371	700	1255	182	36	27	22	72
2	0.20	80	204	400	1275	185	34	25	50	122

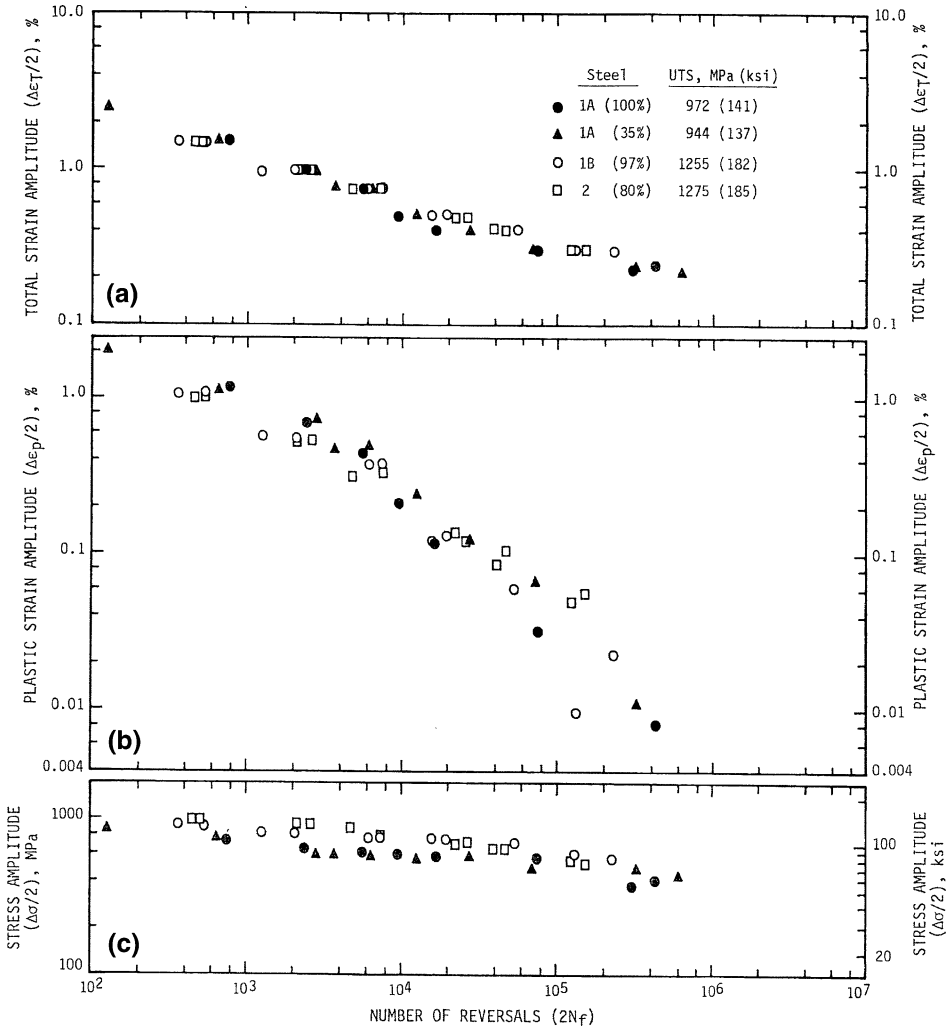

Fig. 10 Fatigue results for quenched and tempered steels. Numbers in parentheses are martensite contents

Table 5 Fatigue life regression constants for quenched and tempered steels

			Fatigue strength						Fatigue ductility (a)		
			UTS		Coefficient, σ_f'						
Steel	Mo, %	Martensite at bar center in as-quenched condition, %	MPa	ksi	MPa	ksi	Exponent, b	Coefficient of determination, r^2	Coefficient, ε_f'	Exponent, c	Coefficient of determination, r^2
1A	0.36	100	972	141	1089	158	−0.065	0.921	3.029	−0.797	0.969
1A	0.36	35	944	137	1165	169	−0.074	0.931	0.872	−0.652	0.931
1B	0.38	97	1255	182	1386	201	−0.067	0.932	0.491	−0.604	0.957
2	0.20	80	1275	185	2096	304	−0.110	0.937	0.303	−0.536	0.981

(a) Includes only those specimens which had a $\Delta\varepsilon_p/2 > 0.01\%$

Table 6 Calculated fatigue life for quenched and tempered steels at various levels of cyclic strain

			UTS		Calculated fatigue life (N_f) at total strain amplitudes ($\Delta\varepsilon_T/2$) of:				
Steel	Mo, %	Martensite at bar center in as-quenched condition, %	MPa	ksi	±1.3%	±0.9%	±0.6%	±0.45%	±0.25%
1A	0.36	100	972	141	675	1,275	2,950	6,000	125,000
1A	0.36	35	944	137	500	1,090	2,950	7,000	125,000
1B	0.38	97	1255	182	395	1,000	3,600	12,500	1,715,000
2	0.20	80	1275	185	426	1,190	4,550	14,500	380,000

Table 7 Monotonic and cyclic stress-strain behavior of quenched and tempered steels

			Monotonic							Cyclic				
			YS		UTS		Strength Coefficient, K			YS		Strength coefficient, K'		
Steel	Mo, %	Martensite at bar center in as-quenched condition, %	MPa	ksi	MPa	ksi	MPa	ksi	Strain Hardening Exponent, n	MPa	ksi	MPa	ksi	Strain hardening exponent, n'	Coefficient of determination, r^2
1A	0.36	100	896	130	972	141	903	131	0.011	558	81	1517	220	0.164	0.998
1A	0.36	35	758	110	944	137	1448	210	0.099	558	81	1572	228	0.171	0.994
1B	0.38	97	1124	163	1255	182	1613	234	0.059	...	...	1434	208	0.102	0.916
2	0.20	80	972	141	1275	185	2323	337	0.152	...	...	2640	383	0.203	0.936

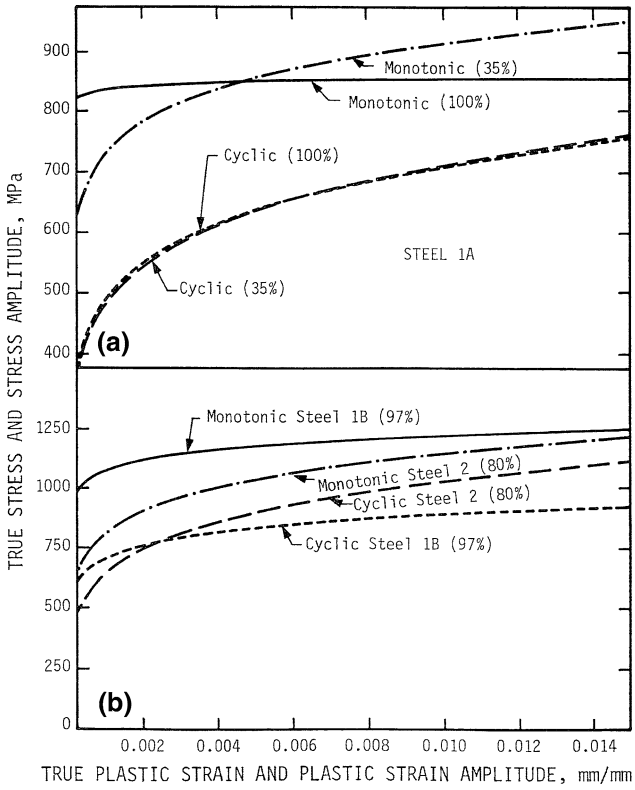

Fig. 11 Monotonic and cyclic stress-strain curves for quenched and tempered steels. Numbers in parentheses are martensite contents

on tempering would then correspond to relief of these stresses (Ref 14).

Mechanical test results (Ref 12, 15) have confirmed that low stresses are responsible for the initial plastic deformation of as-quenched ferrous martensite because martensitic transformation develops residual internal stresses. Unless transformation to bainite also develops these internal stresses, the higher as-tempered versus as-quenched YS of some conditions in this study would not be explained. The conversion of retained austenite to martensite on tempering is one other possible explanation for the increase in YS on tempering the steels with less than 100% as-quenched martensite.

As a general rule, more desirable tensile properties will be obtained after tempering with higher martensite content after quenching. After tempering to an UTS specification, steel sections that had been quenched to higher martensite contents will possess higher yield strengths and similar tensile ductilities as compared to steel sections with lower martensite contents.

4.2 Impact Toughness After Tempering

Tempering at higher temperatures usually results in better toughness and lower strength (Ref 1). Table 4 and Fig. 8 show that this generally accepted trend is operative for the 50% martensite content condition in this study. Tempering at 538 °C (1000 °F) resulted in significantly higher absorbed energies and a lower FATT (in addition to a lower UTS) when compared to tempering at 399 °C (750 °F).

Q&T low alloy steels can be embrittled during tempering. However, none of the various types of embrittlement probably played a role in the experiments described in this paper. Table 4 shows that CVN toughness was obtained for specimens

tempered at temperatures beyond the extremes of the temperature ranges where susceptibility to "tempered martensite embrittlement" (TME) or "temper embrittlement" (TE) reportedly occur. TME and TE occur after service or tempering exposure between 204 and 371 °C (400 and 700 °F) (Ref 13, 16). The aluminum contents of the three experimental steels (Table 1) are in the range stated to be helpful (Ref 16) for increasing resistance to TME. The 0.2% carbon content, short tempering time (2 h), thin sections [maximum of 25 mm (1 in.) diameter], and the 0.2-0.38%Mo content used in this study are all contrary to trends stated (Ref 13, 16) to enhance TE susceptibility. "Blue brittleness" is not indicated since no significant losses in tensile ductility were obtained.

Figure 8 demonstrates that better strength-toughness combinations can be achieved with higher martensite contents at all strength levels. When compared at a UTS of approximately 965 MPa (140 ksi), a change in martensite content of 35-100% resulted in substantial decrease in fracture appearance transition temperature, FATT. If the 100% martensite content [UTS = 972 MPa (141 ksi)] is compared to the 50% martensite content at both its strength levels [UTS = 869 and 1144 MPa (126 and 165 ksi)], the fully martensitic structure resulted in higher toughness. If the toughness of the 35% martensite condition is compared to that of the two 50% martensite strength conditions, the higher martensite content resulted in a lower FATT at both higher and equivalent levels of UTS and YS.

A comparison of the results obtained for the 97% martensite condition with those obtained for the 50% martensite condition at the same FATT illustrates that at equivalent toughness, higher yield and tensile strengths can be obtained with a higher martensite content. At a UTS near 1240 MPa (180 ksi), a change in martensite content from 80 to 97% resulted in a relatively small decrease in the FATT. However, when this improvement in toughness is considered in conjunction with the 152 MPa (22 ksi) higher YS of the 97% versus 80% martensite conditions, the improvement in toughness obtained with the higher martensite and molybdenum contents is more impressive.

The low toughness in steels having mixed microstructures can be correlated with the non-martensitic constituents. In continuous-cool, slack quench heat treatments, such as those performed for all but the fully martensitic condition in this study, a number of different constituents can nucleate at different temperatures on cooling. Figures 2(b, c) and 3(a, b) show that the microstructures of all these slack-quenched steels exhibit upper bainite. This upper bainite is believed to be responsible for lower toughness, i.e., the more upper bainite, the higher the impact transition temperature.

This observation is consistent with the results of earlier experiments performed on 4340 steel (Ref 1, 17). Isothermal heat treatments which produced an upper bainite microstructure resulted in low YS, low tensile ductility, and poor impact toughness (Ref 1). In contrast, earlier results also indicated that austempering (isothermal formation) to lower bainite resulted in equivalent or slightly superior mechanical properties as compared to fully martensitic microstructures (Ref 2, 17). Therefore, the conclusions reached in this study must pertain only to mixed microstructures containing upper bainite produced by continuous cooling heat treatments. In any event, austempering (isothermal transformation to lower bainite) of large sections manufactured from low or medium carbon alloy steels must be controlled carefully because it may not be possible to quench fast enough to prevent the formation of significant amounts of upper bainite.

Toughness losses are occasionally associated with higher alloying additions. For example, chromium raises the ductile-to-brittle transition temperature slightly (Ref 1) and can aggravate tendencies toward TE (Ref 1, 16). However, addition of elements such as chromium, nickel, and molybdenum control toughness more through their effects on microstructure (Ref 1). Increasing alloy content to enhance hardenability and ensure fully martensitic as-quenched microstructures allows the selection of higher tempering temperatures, thus resulting in improved toughness.

4.3 Fatigue Life After Tempering

Although low cycle fatigue resistance was unaffected by variations in as-quenched martensite content, Fig. 10 and Table 6 show that actual and predicted fatigue life in the high cycle regime ($>10^4$ cycles) increased with higher martensite contents for the high UTS level [1240 MPa (180 ksi)]. This result agrees earlier observations (Ref 4) of decreased fatigue limits with decreased martensite content in 0.4%C steels.

4.4 Strain Hardening Behavior After Tempering

Figure 11(a) shows that the fully martensitic condition exhibited virtually no monotonic work hardening. This is similar to the result obtained for a fully martensitic Fe-0.2C alloy after tempering at 400 °C (752 °F) (Ref 12). The microstructure was probably responsible for the large differences in as-tempered work hardening behavior obtained in this study 35 and 100% martensite contents. The bainitic ferrite shown in Fig. 4(c), which was present in the as-quenched condition as shown in Fig. 2(c), might have work hardened significantly when compared to the lath packets shown in Fig. 4(a), obtained after tempering the fully martensitic condition.

Packet size affects the strength of as-quenched martensites in a manner similar to the effect of ferrite grain size on the strength of ferritic steels, but martensite steels that work harden significantly after quenching no longer do so after tempering (Ref 12). Figures 11(a, b) show a similar (flat) trend in as-tempered monotonic work hardening behavior for the 97% and 100% martensite contents. In addition, the 97% martensite condition (Steel 1B) work hardened more than the fully martensitic condition (Steel 1A). Since Fig. 3 and 5 show that the 35 and 80% martensite specimens contained bainitic ferrite, the pronounced work hardening (see Fig. 11a, b) obtained for these two conditions could be associated with bainitic ferrite too.

Figure 11 shows that all four conditions exhibited cyclic softening, i.e., the cyclic stress amplitude was lower than the monotonic true stress for any plastic strain up to 1.5%. This observation is consistent with the behavior associated with Q&T steels as a class of materials (Ref 5).

Unlike the differences in monotonic work hardening behavior for the 35 and 100% martensite conditions discussed above, Fig. 11(a) shows that the two conditions had identical cyclic stress-strain curves. Although the monotonic offset YS was higher for the 100% martensite content, Table 6 shows that the 35% martensite content possessed an identical cyclic YS. No cyclic YS was determined for the 80 and 97% martensite conditions because ISTs were not performed. However, Fig. 11 shows that higher cyclic flow stresses were obtained at all levels of applied plastic strain between 0.2 and 1.5% for the

two conditions possessing the higher UTS of 80 and 97% martensite. Therefore, the trends in cyclic YS and UTS were similar and not a function of martensite content.

5. Conclusions

High toughness and strength-toughness combinations after tempering were achieved with steels having high as-quenched martensite contents. A range of different as-quenched martensite contents (35, 50, and 100%) was established in a 0.23C-0.81Mn-0.51Ni-0.51Cr-0.36Mo steel by varying section size and quenching media.

After tempering to the same UTS, the fully martensitic condition exhibited a significantly higher YS, higher impact energies, and lower FATT than the 35% martensite condition. Toughness was directly related to martensite content based on comparisons of the 35, 50, and 100% martensite contents at all levels of as-tempered ultimate tensile strengths.

Martensite contents were also varied by quenching two 0.21C-0.82Mn-0.55Ni-0.50Cr steels with differing molybdenum contents (0.2 and 0.38%) in the same section size. The 0.38%Mo steel with 97% martensite exhibited a higher YS and higher toughness than the 0.2%Mo steel with 80% martensite, after tempering to the same UTS.

The low cycle fatigue life of the Q&T steels was not a function of as-quenched martensite content. All combinations of steels/heat treatments exhibited cyclic softening, and the cyclic YS was independent of martensite content. The cyclic flow strength, however, was higher for the conditions exhibiting higher tensile strengths, but again, independent of the percent martensite present.

At one of the two tensile strength levels evaluated, the predicted high cycle fatigue life increased with martensite content. Increasing the molybdenum content from 0.2 to 0.38% increased the amount of martensite in the microstructure and resulted in higher predicted high cycle fatigue life.

Appendix

Relevant Fatigue and Strain Hardening Equations and Symbols

The total strain amplitude $(\Delta\varepsilon_T/2)$ was the controlled variable in the fatigue tests. The total strain amplitude was equated to the sum of its elastic $(\Delta\varepsilon_e/2)$ and plastic $(\Delta\varepsilon_p/2)$ components, i.e.,

$$(\Delta\varepsilon_T/2) = \Delta\varepsilon_e/2 + \Delta\varepsilon_p/2 \quad \text{(Eq 1)}$$

The elastic strain amplitude was calculated using Hooke's Law (E = Young's or elastic modulus) and the saturation stress amplitude $(\Delta\sigma/2)$ obtained at half-life (0.5 N_f) as follows:

$$\Delta\varepsilon_e/2 = \Delta\sigma/2E \quad \text{(Eq 2)}$$

The plastic strain amplitude $(\Delta\varepsilon_p/2)$ was calculated by subtraction, i.e.,

$$\Delta\varepsilon_p/2 = \Delta\varepsilon_T/2 - \Delta\varepsilon_e/2 = \Delta\varepsilon_T/2 - \Delta\sigma/2E \quad \text{(Eq 3)}$$

The saturation stress $(\Delta\sigma/2)$ and the plastic strain $(\Delta\varepsilon_p/2)$ amplitudes were related to the number of reversals $(2N_f)$ by

$$\Delta\sigma/2 = \sigma'_f(2N_f)^b \quad \text{(Eq 4)}$$

and

$$\Delta\varepsilon_p/2 = \varepsilon'_f(2N_f)^c \quad \text{(Eq 5)}$$

where the four constants σ_f, b, ε'_f, and c are the fatigue strength coefficient, fatigue strength exponent, fatigue ductility coefficient, and the fatigue ductility exponent respectively, determined using linear regression. The above equations were combined to obtain the overall total strain amplitude-life equation.

$$\Delta\varepsilon_T/2 = (\sigma'_f/E)(2N_f)^b + \varepsilon'_f(2N_f)^c \quad \text{(Eq 6)}$$

The monotonic and cyclic stress-plastic strain behavior of the steels was characterized using the equation

$$\sigma = K\varepsilon_p^n \quad \text{(Eq 7)}$$

and

$$\Delta\sigma/2 = K'(\Delta\varepsilon_p/2)^{n'} \quad \text{(Eq 8)}$$

where K is the monotonic strength coefficient, n is the monotonic strain hardening exponent, σ is the true tensile stress, ε_p is the true plastic tensile strain, K' is the cyclic strength coefficient, and n' is the cyclic strain hardening exponent. The four constants (K, n, K', and n') were determined using linear regression. (The above Eqs 4, 5, 7, and 8 in the form of $y = Ax^B$ were transformed to $\log y = \log A + B \log x$ for the purposes of obtaining the linear regression constants A and B.) A material is considered as cyclically softening when the cyclic stress amplitude is lower than the monotonic true stress, i.e., $\Delta\sigma/2 < \sigma$, for a given plastic strain; cyclic hardening is the opposite situation.

References

1. G.J. Roe and B.L. Bramfitt, Notch Toughness of Steels, *ASM Handbook: Properties and Selection: Irons, Steels, and High-Performance Alloys*, 10th ed., Vol. 1, ASM International, Materials Park, OH, 1990, p 748, which cites the original paper: R.F. Hehemann, V.J. Luhan, and A.R. Troiano, The Influence of Bainite on Mechanical Properties, *Trans. ASM*, 1957, **49**, p 409–426
2. J.M. Tartaglia, K.A. Lazzari, G.P. Hui, and K.L. Hayrynen, A Comparison of Mechanical Properties and Hydrogen Embrittlement Resistance of Austempered versus Quenched & Tempered 4340 Steel, *Metall. Mater. Trans.*, 2008, **39A**(3), p 559–576
3. R. W. Landgraf, Fatigue Resistance and Microstructure of Ferrous Alloys, *ASM Handbook: Fatigue and Fracture*, 10th ed., Vol. 19, ASM International, Materials Park, OH, 1996, p 608
4. F. Borik, R.D. Chapman, and W.E. Jominy, The Effect of Per Cent Tempered Martensite on Endurance Limit, *Trans. ASM*, 1958, **50**, p 242–254
5. R.W. Landgraf, Control of Fatigue Resistance Through Microstructure, *Fatigue and Microstructure*, American Society for Metals, Metals Park, OH, 1979, p 439–466
6. N.S. Stoloff and D.J. Duquette, Microstructural Effects in the Fatigue Behavior of Metals and Alloys, *CRC Critic. Rev. Solid State Sci.*, 1974, **4**(4), p 615–687
7. J.M. Tartaglia and G.T. Eldis, Core Hardenability Calculations for Carburizing Steels, *Metall. Trans.*, 1984, **15A**(6), p 1173–1183
8. C.A. Siebert, D.V. Doane, and D.H. Breen, Metallurgical Factors Influencing Hardenability of Steel, *The Hardenability of Steels*, American Society for Metals, Metals Park, OH, 1977, p 100ff
9. D.T. Raske and J. Morrow, *Manual on Low Cycle Fatigue Testing, STP 465*, American Society for Testing and Materials, Philadelphia, PA, 1969, p 12

10. J.M. Hodge and M.A. Orehoski, Relationship Between Hardenability and Percentage of Martensite in Some Low Alloy Steels, *Trans. AIME*, 1946, **167**, p 627–638
11. G. Krauss, Martensitic Transformation, Structure and Properties in Hardenable Steels, *Hardenability Concepts with Applications to Steel*, The Metallurgical Society of AIMS, Warrendale, PA, 1978, p 229–245
12. T. Swarr and G. Krauss, The Effect of Structure on the Deformation of As-Quenched and Tempered Martensite in an Fe-0.2 Pct C Alloy, *Met. Trans. A*, 1976, **7A**, p 41–48
13. G. Krauss, Low Toughness and Embrittlement Phenomena in Steels, Chap 19, *Steels: Processing, Structure and Performance*, ASM International, Materials Park, OH, 2005, p 396-404
14. H. Muir, B.L. Averbach, and M. Cohen, The Elastic Limit and Yield Behavior of Hardened Steels, *Trans. ASM*, 1955, **47**, p 380
15. C.L. Magee and H.W. Paxton, Experimental Support for "Hard" Martensite, *Trans. TMS-AIME*, 1968, **242**, p 1766–1767
16. J.R. Low, Jr., Embrittlement of Steels, *ASM Metals Handbook: Properties and Selection: Irons and Steels*, 9th ed., Vol. 1, American Society for Metals, Metals Park, OH, 1978, p 683–688,
17. Y. Tomita and K. Okabayashi, Improvement in Lower Temperature Mechanical Properties of 0.40 Pct C-Ni-Cr-Mo Ultrahigh Strength Steel With the Second Phase Lower Bainite, *Met. Trans. A*, 1983, **14A**, p 485–492